Supplementary materials

Anonymous Author(s)
Affiliation
Address
email

1 Proof of Eq. 8

$\phi(G,F) \leq \|\delta_\tau(F)\|_0 \ll \|\delta_{2\tau}(\mathbf{I}_D)\|_0 \ - \ \|\delta_\tau(\mathbf{k}_p)\|_0 \leq \phi(\mathbf{k}_p, \mathbf{I}_D)$

$$\begin{aligned}
\phi(G,F) &= \sum_{i,j} sign(\delta_\tau(G_{ij} - F_{ij})) && (1)\\
&= \sum_{i,j} sign(\delta_\tau(F_{ij}S_{ij} - F_{ij})) && (2)\\
&= \sum_{F_{ij}<\tau} sign(\delta_\tau(F_{ij}S_{ij} - F_{ij})) + \sum_{F_{ij}\geq\tau} sign(\delta_\tau(F_{ij}S_{ij} - F_{ij})) && (3)\\
&\leq \sum_{F_{ij}<\tau} sign(\delta_\tau(F_{ij}(S_{ij} - 1))) + \sum_{F_{ij}\geq\tau} sign(\delta_\tau(F_{ij})) && (4)\\
&= 0 + \sum_{F_{ij}\geq\tau} sign(\delta_\tau(F_{ij})) && (5)\\
&= \|\sigma_\tau(F)\|_0 && (6)
\end{aligned}$$

$$\begin{aligned}
\phi(k_p, I_D) &= \sum_{i,j} sign(\delta_\tau([k_p]_{ij} - [I_D]_{ij})) && (7)\\
&= \sum_{[k_p]_{ij}>\tau} sign(\delta_\tau([k_p]_{ij} - [I_D]_{ij})) + \sum_{[k_p]_{ij}<\tau} sign(\delta_\tau([k_p]_{ij} - [I_D]_{ij})) && (8)\\
&\geq \sum_{[k_p]_{ij}<\tau} sign(\delta_\tau([k_p]_{ij} - [I_D]_{ij})) && (9)\\
&\geq \sum_{[k_p]_{ij}<\tau, [I_D]_{ij}>2\tau} sign(\delta_\tau([k_p]_{ij} - [I_D]_{ij})) && (10)\\
&\geq \|\sigma_{2\tau}(I_D)\|_0 - \|\delta_\tau(k_p)\|_0 && (11)
\end{aligned}$$

where both F and k_s are sparse such that $\|\sigma_\tau(F)\|_0$ and $\|\delta_\tau(k_p)\|_0$ are significantly smaller than $\|\sigma_{2\tau}(I_D)\|_0$ due to the non-sparsity of I_D. So we come to $\phi(k_p, I_D) \gg \phi(G,F)$.

2 Fourier transform of 2D-Gaussian function.

(1) For the two-dimensional Gaussian function $f(x,y)$,

$$f(x,y) = \frac{e^{-(\frac{x^2}{\sigma_x{}^2} + \frac{y^2}{\sigma_y{}^2})}}{2\pi\sigma_x\sigma_y} \tag{12}$$

Submitted to 35th Conference on Neural Information Processing Systems (NeurIPS 2021). Do not distribute.

where σ_x and σ_x is the variance in two orthogonal directions respectively. After two-dimensional Fourier transform:

$$F(u,v) = \sum_x \sum_y f(x,y) e^{-j2\pi(ux+vy)} \tag{13}$$

$$= e^{-2\pi^2(\sigma_x^2 u^2 + \sigma_y^2 v^2)} \tag{14}$$

$$= Ae^{-(\frac{u^2}{2\sigma_u^2} + \frac{v^2}{2\sigma_v^2})} \tag{15}$$

$$\sigma_u \propto \frac{1}{\sigma_x}, \sigma_v \propto \frac{1}{\sigma_y} \tag{16}$$

Where σ_u and σ_v denote the new variance of the Gaussian function after transformation. Discrete Fourier Transform (DFT) result $F_g(u,v)$ for *Gaussian kernel* is also in *Gaussian form*, and their variances are in *inverse proportion* [1].

3 Limitations

(1) As described in Section 3.1 of this paper, same with most previous blind SR methods, our method is also based on convolution and downsampling degradation model to describe the real degradation process, which is the commom setting. But this description may not cover all forms of degradation, such as non-uniform degradation (kernel each local area may be different) and motion synthesis using aliasing of adjacent frames. This needs further research and exploration in future work.
(2) Compared with the previous work, we provide a more accurate and efficient blind blur kernel estimation scheme. Combined with the existing efficient non-blind SR methods, we achieve the best blind SR results. Since the proposed estimation scheme is task independent and we mainly focus on blind-SR, it may also be suitable for some other blind task scenarios such as deblurring, which needs more future exploration.

4 More quantitative and visual results

In addition to the fidelity-oriented blind-SR experiment in the main text, we conducted additional perceptual-oriented experiments. Same as the previous experimental setup, we use ESRGAN and LPIPS perceptual metric to compare the results of $2\times, 3\times, 4\times$ blind-SR results on LR images from DIV2K degraded by random Gaussian kernels, as shown in the Table 1.

Method	DIV2K			Flicker2K		
	2x	3x	4x	2x	3x	4x
ESRGAN	0.4969	0.5757	0.6315	0.4881	0.5719	0.6269
FCA	0.2799	0.3527	0.3818	0.2627	0.3488	0.3661
KernelGAN	0.2275	0.3159	0.5774	0.2371	0.3331	0.6141
Ours	0.1968	0.2569	0.3390	0.1987	0.2706	0.3400

Table 1: Quantitative [LPIPS↓] comparison of perception-oriented SR results for $2\times$, $3\times$, $4\times$ up-sampling respectively. The best performance is shown in red and the second best is blue.

Here we also provide a comparison of blind SR performance on the additional synthetic dataset L20 in Table 2. And more visual comparison with state-of-the-art methods as provided and shown in Figure 1, 2, 3 and Figure 5, we show the visual contrast of the *best* methods.

5 Code, data, and instructions needed to reproduction

We provide the code, instructions and dataset with download address for reproduction in the attached zip file.

[1] Reflect in the major and minor axis of the projection boundary on the position coordinate plane

Method	Kernel	L20		
		2x	3x	4x
RCAN finetuned	G	27.05 / 0.7310	24.78 / 0.6569	23.68 / 0.6220
ZSSR		27.00 / 0.7308	24.76 / 0.6569	23.66 / 0.6222
DeblurGAN w. RCAN		27.63 / 0.7516	25.30 / 0.6710	24.03 / 0.6301
KernelGAN		27.39 / 0.7349	25.02 / 0.6649	24.38 / 0.6389
FCA w.RCAN		31.06 / 0.8607	28.07 / 0.7743	26.25 / 0.7107
IKC		29.86 / 0.8670	28.80 / 0.7895	27.10 / 0.7348
S2K w. SFTMD		32.26 / 0.8803	28.95 / 0.7909	27.51 / 0.7361
S2K w.RCAN		32.73 / 0.8838	29.35 / 0.7939	27.83 / 0.7355
RCAN finetuned	M	24.88 / 0.6775	23.04 / 0.6158	22.02 / 0.5906
DeblurGAN w. RCAN		24.77 / 0.6830	23.03 / 0.6179	21.90 / 0.5897
ZSSR		24.85 / 0.6756	23.02 / 0.6151	22.02 / 0.5903
KernelGAN		24.16 / 0.6365	22.85 / 0.6057	21.10 / 0.5418
IKC		27.57 / 0.7901	23.53 / 0.6575	22.60 / 0.6187
Pan *et al.* w.SFTMD		22.63 / 0.6312	21.19 / 0.5647	19.84 / 0.5411
S2K w. SFTMD		32.95 / 0.9070	30.92 / 0.8551	28.36 / 0.7842

Table 2: **Quantitative [PSNR↑ / SSIM↑] comparison results of fidelity-oriented SR model for $2\times$, $3\times$, $4\times$ up-sampling.** G, M denote Gaussian kernels and motion kernels respectively. The best performance is shown in red and the second best in blue.

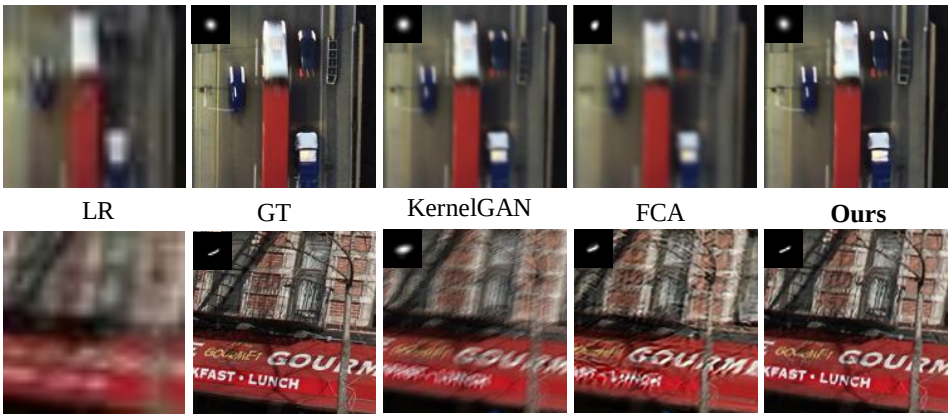

Figure 1: $2\times$ blind SR results for LR degraded with unknown kernel from DIV2K. For FCA is not able to handle motion kernel, so we use Pan *et al.*'s as a comparison instead. Due to more accurate kernel estimation, our method achieves the most pleasant results compared with other methods.

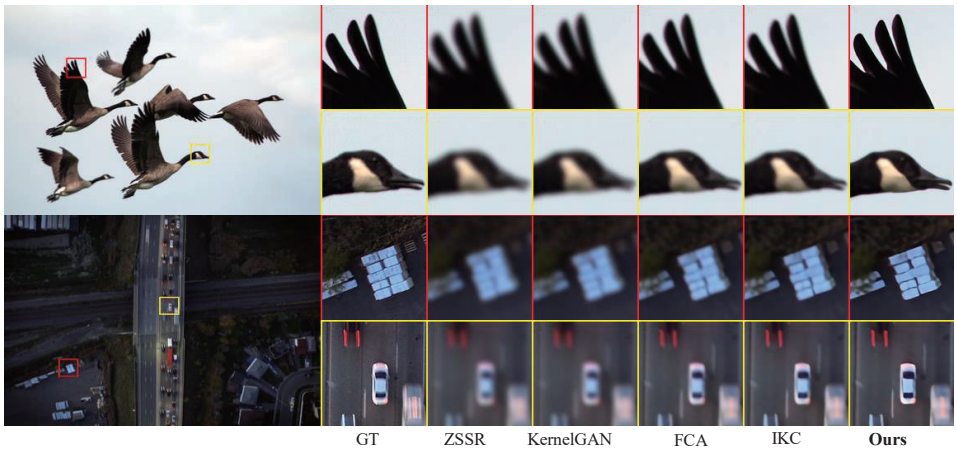

Figure 2: $2\times$ blind SR results for LR degraded with unknown Gaussian kernel from DIV2K.

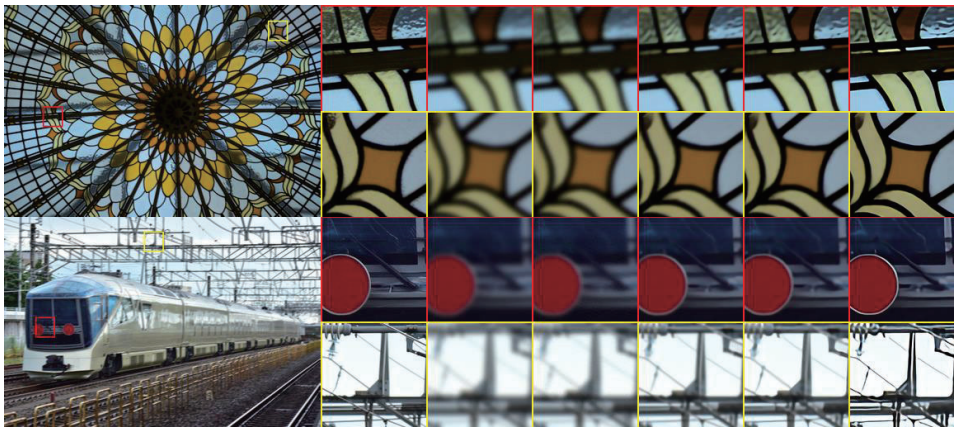

Figure 3: 2× Blind SR results for LR degraded with unknown Gaussian kernel from DIV2K.

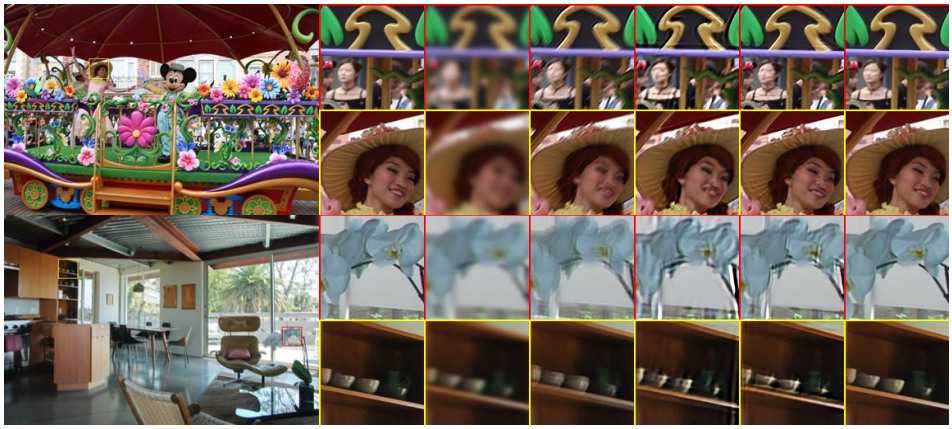

Figure 4: 2× Blind SR results for LR degraded with unknown motion kernel from Flicker2K.

Figure 5: 2× Blind SR results for LR degraded with unknown motion kernel from Flicker2K.